ACS Macro Letters

Letter

pubs.acs.org/macroletters

Polymer Side Chain Modification Alters Phase Separation in Ferroelectric-Semiconductor Polymer Blends for Organic Memory

Gregory M. Su,[†] Eunhee Lim,[†] Andrew R. Jacobs,[†] Edward J. Kramer,[†,‡] and Michael L. Chabinyc*,[†]

[†]Materials Department and [‡]Department of Chemical Engineering, University of California Santa Barbara, Santa Barbara, California 93106, United States

Supporting Information

ABSTRACT: Side chain modification of a semiconducting polythiophene changes the resulting phase separation length scales when blended with a ferroelectric polymer for use in organic ferroelectric resistive switches. The domain size of the semiconducting portion of blends of poly[3-(ethyl- 5-pentanoate)thiophene-2,5-diyl] (P3EPT) and poly(vinylidene fluoride-*co*-trifluoroethylene) (PVDF-TrFE) in thin film blends are smaller than previously reported and easily controllable in size through simple tuning of the weight fraction of the semiconducting polymer. Furthermore, P3EPT has a relatively high degree of crystallinity and bimodal crystallite orientations, as probed by wide-angle X-ray scattering. Resistive switches fabricated from blends of P3EPT and PVDF-TrFE show memristive switching behavior over a wide range of polythiophene content and good ON/OFF ratios.

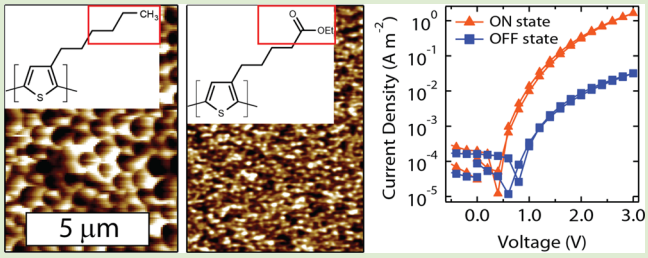

Polymers offer a unique platform for creating low-cost, solution-processable, and flexible electronics.[1−5] Semiconducting polymers are essential for these applications, but ferroelectric polymers have also proven to be useful as well. For example, ferroelectric polymers have been shown to increase the power conversion efficiency of organic photovoltaics.[6−10] One application, in particular, that has been of recent interest is organic-based nonvolatile memory devices,[11−13] including ferroelectric transistors and diodes.[14,15]

The working mechanism of organic ferroelectric devices relies on the fact that certain polymers, such as those based on poly(vinylidene fluoride), have intrinsic permanent dipole moments that can be oriented by an applied electric field, leading to ferroelectric behavior.[16,17] Ferroelectric resistive switches can be fabricated by blending a ferroelectric polymer and a semiconducting polymer, first demonstrated by Asadi et al.[18] Because dissimilar polymers phase separate, thin films of blends have distinct ferroelectric and semiconducting regions. Understanding how this phase separation occurs during solidification and subsequent processing is important because the morphology defines the pathways for charge transport and the switching characteristics.

Blends of ferrorelectric polymers and semiconducting polymers provide an interesting opportunity to examine fundamental processes of phase separation in thin films of semicrystalline polymers from solution. Here, we examine the effects of altering the side chain structure of the semiconducting polymer on the phase separation and molecular order in a ferroelectric-semiconductor polymer blend. We find that modification of side chains is a useful route to achieve reliable nanoscale phase separation in thin films while maintaining ferroelectric switching behavior.

The operation of ferroelectric diodes depends critically on the morphology of the phase separated ferroelectric-semiconductor blend film. Charge carriers only travel through the semiconducting polymer, and the ferroelectric polymer determines the switching behavior of the device. It is believed, based on experimental data and device models, that the stray field of the positively (negatively) poled ferroelectric polymer lowers (increases) the barrier to charge injection into the semiconductor phase, resulting in greater (decreased) current in the ON (OFF) state.[19,20] The charge carriers travel predominantly near the semiconductor-ferroelectric domain interfaces.[21] Semiconductor domains that are too large will reduce the interfacial area of the domains and the overall current. On the other hand, the stray field lines of the poled ferroelectric act against the direction of charge transport, and this can reduce the current if semiconductor domains are too small. A competition between these two effects results in an optimum lateral size for the semiconductor domains, suggested to be about 50−100 nm.[20] Therefore, an optimal device would have as large a volume fraction as possible of ∼50 nm size domains of semiconducting polymer surrounded by ferroelectric polymer domains (the minimum size of the ferroelectric domains has not yet been studied).

A well-defined phase separated structure with easily tunable domain sizes is required for better understanding of fundamental links between morphology and electrical properties. It is difficult to predict polymer−polymer interaction

Received: September 6, 2014
Accepted: November 10, 2014
Published: November 19, 2014

parameters, making it challenging to reduce the domain size of polythiophene based blends well below even a micron when relying on spontaneous phase separation,[22] and previous work that utilized regio-irregular poly(3-hexylthiophene) (rir-P3HT) blended with the typical ferroelectric polymer, poly(vinylidene fluoride-*co*-trifluoroethylene) (PVDF-TrFE), showed large-scale phase separation between polymers.[22] Top-down physical patterning methods such as nanoimprint lithography can be used to achieve higher storage densities and smaller switching voltages,[23] however, such additional processing steps would complicate large-scale production of these devices using printing methods. Semiconducting polymers other than polythiophenes can also be used, and proper choice of solvent and deposition method can produce smoother, thinner films with reduced switching voltages.[24] Incorporation of an insulating, amorphous polymer can also improve the ferroelectric and dielectric performance of ferroelectric polymers.[25]

In order to tune the phase separation of ferrelectric-semiconductor polymers blends, we sought to modify the polymer−polymer interactions. It is important to choose a polymer that has a low surface interaction energy with PVDF-TrFE, because a thermal annealing step is required after deposition of the polymer blend film that could lead to coarsening. There is a certain degree of phase separation that occurs during solvent evaporation and solidification of the films during the spin coating process. However, good working devices cannot be made from as-cast films because the paraelectric α-phase of PVDF-TrFE is more stable at room temperature. In order to achieve this, we looked to use a semiconducting polymer that would potentially have more favorable polymer−polymer interactions with PVDF-TrFE. It is known that PVDF has a compatible Flory−Huggins interaction parameter with poly(methyl methacrylate) (PMMA).[26,27] In an effort to alter polymer−polymer interactions but maintain semiconducting and charge transport properties, a side chain structure was chosen that is similar to PMMA, while keeping the semiconducting thiophene backbone. The polythiophene used in this study is poly[3-(ethyl-5-pentanoate)thiophene-2,5-diyl], which will be referred to as P3EPT, shown in Figure 1. P3EPT is expected to have relatively similar electronic properties to P3HT, and thin film UV−vis absorption shows a slight blue shift compared to P3HT (Supporting Information).

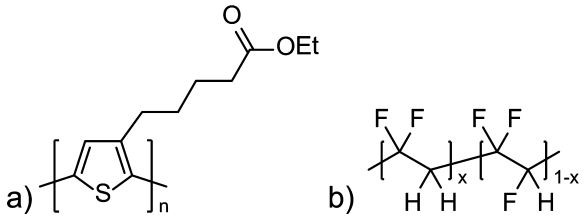

Figure 1. Chemical structures of (a) P3EPT and (b) PVDF-TrFE.

Blending P3EPT with PVDF-TrFE leads to small domain sizes. Morphology characterization was performed on blends of P3EPT and PVDF-TrFE that were dissolved together in a common solvent (ranging from 10 to 50 wt % P3EPT) and spin coated into thin films, followed by postdeposition thermal annealing at 135 °C, close to the crystallization temperature of PVDF-TrFE,[28] for 3 h and subsequent slow cooling to room temperature. This annealing step is required to stabilize and enhance the crystallinity of the ferroelectric β-phase of PVDF-TrFE. P3EPT based blends exhibit much smaller polythiophene domain sizes for a given blend ratio compared to blends of PVDF-TrFE and other semiconducting polymers such as regioregular P3HT (Figure 2), rir-P3HT,[22] or poly[(9,9-dinoctylfluorenyl-2,7-diyl)-*alt*-(benzo[2,1,3]thiadiazol-4,8-diyl)] (F8BT).[21] The phase separation at the film surface can be probed by atomic force microscopy (AFM), and it is clear that P3EPT-based films not only have smaller domains for a given weight fraction of polythiophene, but also a much smoother film surface compared to blends based on P3HT, as shown in Figure 2a−c. These are already notable advancements since the ideal semiconductor domain size is thought to be on the order of ∼50−100 nm, and it is often difficult to form smooth films of PVDF-TrFE via spin coating due to the large crystallites that can form, typically requiring more involved strategies such as rapid thermal treatment or blending with PMMA to reduce film roughness.[29,30]

To examine the origin of the observed domain structure, thin films of P3EPT:PVDF-TrFE were spun cast from solutions of varying weight % of P3EPT. AFM images clearly show that increasing the fraction of P3EPT results in an increase in domain size at the film surface, and this is shown in Figure 2d−f. The linear dependence of P3EPT domain size with P3EPT wt % (Figure 2g) suggests that the phase-separated structure may form due to spinodal decomposition, as opposed to nucleation and growth, similar to what has been observed in other PVDF-TrFE:semiconducting polymer blends.[22,24] It is assumed that the regions of higher phase angle correspond to P3EPT domains since they increase in size with P3EPT content. A similar trend is seen in the AFM height topography as shown in the Supporting Information. AFM height profiles reveal that some P3EPT domains are convex, and protrude out from the film surface, while others are concave depressions. This may have an important impact on electrical properties. It has been shown in an F8BT:PVDF-TrFE system that convex semiconductor domains contribute much less current compared to concave domains, and convex domains are therefore undesirable. This is possibly due to a thin layer of PVDF-TrFE that may form on the bottom, buried interface of convex semiconductor domains, blocking charges from being injected into the semiconductor.[21]

P3EPT and PVDF-TrFE are not completely miscible because a distinct phase-separated structure forms in the blend, but interactions between the polymers could affect crystallite formation, and can be probed through thermal analysis. Differential scanning calorimetry (DSC) thermograms reveal the main melting and crystallization transitions for P3EPT and PVDF-TrFE (Supporting Information). P3EPT has an endothermic melting transition at around 188 °C and an exothermic crystallization transition at 149 °C. Both of these transitions have two distinct peaks close together, and this is commonly seen for polythiophene derivatives and may be a result of ordering/disordering of two coexisting semicrystalline microstructures that could form during heating and cooling.[31,32] PVDF-TrFE has a main melting endotherm at 151 °C and a crystallization exotherm at 131 °C. There is a noticeable shift in the peak position of the crystallization temperatures for both polymers when blended together (Supporting Information). For example, in a 50:50 P3EPT:PVDF-TrFE blend, the crystallization temperature of P3EPT is lowered by about 7 °C to 142 °C, and the transition for PVDF-TrFe is raised by about 2 °C to 133 °C. A similar trend is seen for other blend ratios. This suggests that mixing makes it more difficult for P3EPT to

dx.doi.org/10.1021/mz5005647 | *ACS Macro Lett.* 2014, 3, 1244−1248

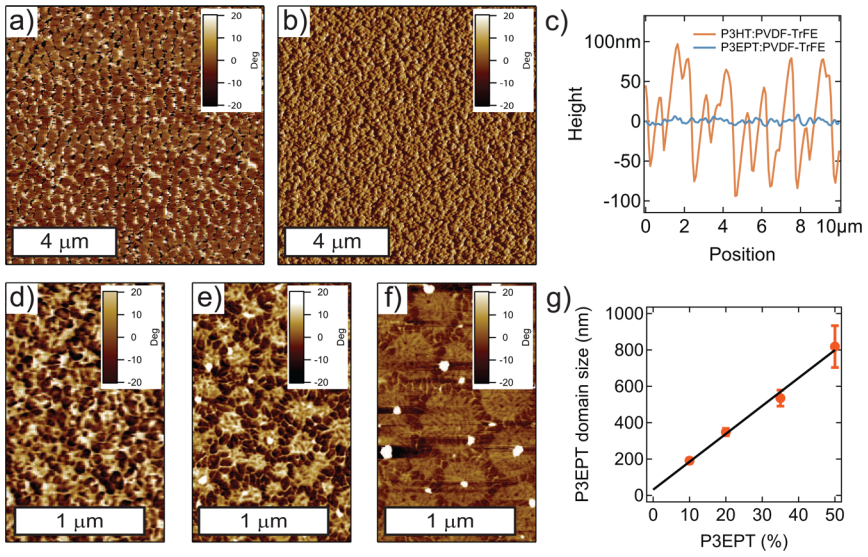

Figure 2. AFM phase images of (a) a 10:90 P3HT:PVDF-TrFE blend and (b) a 10:90 P3EPT:PVDF-TrFE blend which shows much smaller phase separation length scales. Additionally, P3EPT based blends result in much smoother films as shown in (c). The domain size of P3EPT is tunable through variation of P3EPT content, examples of (d) 10 wt %, (e) 20 wt %, and (f) 35 wt % P3EPT are shown. The linear dependence of P3EPT domain size with P3EPT content is shown in (g).

crystallize (greater undercooling required), but once it does crystallize, the domains may promote the formation of PVDF-TrFE crystallites. This differs from both regioregular P3HT and rir-P3HT. Regioregular P3HT has a higher crystallization temperature, around 200 °C,[33] compared to P3EPT, whereas rir-P3HT does not crystallize.

Semiconducting polymers are typically semicrystalline, and this crystallinity can have an impact on charge transport. Therefore, it is important to determine the structural order of P3EPT and to determine if changes in the crystallites occur when it is mixed with PVDF-TrFE, which is also a semicrystalline polymer. Grazing incidence wide-angle X-ray scattering (GIWAXS) was used to probe the crystalline nature of thin films of PVDF-TrFE, P3EPT, and their blends. The 2D GIWAXS pattern of PVDF-TrFE reveals a main scattering reflection at q = 1.41 Å^{-1}, corresponding to a spacing of ∼4.5 Å, similar to previous reports.[22,34] The typical hexagonal structure of the PVDF-TrFE crystallites is also evident in the intensity distribution as a function of polar angle of the scattering peak (Supporting Information). GIWAXS of P3EPT has not been reported previously, and the scattering pattern indicates a relatively crystalline polymer. We assume a similar crystallographic assignment as commonly used for other semiconducting polymers where the a axis is along the side chain stacking and the b axis along the $\pi-\pi$ stacking direction. The 2D GIWAXS of P3EPT shown in Figure 3a depicts three orders of reflections along the side chain stacking direction, which are the (100), (200), and (300) peaks located at 0.34 Å^{-1} (18.8 Å), 0.67 Å^{-1} (9.3 Å), and 1.0 Å^{-1} (6.3 Å), respectively. The d-spacing in the side chain stacking direction is greater than P3HT,[33] as expected, but about 1.5 Å smaller than what has been reported for poly(3-octylthiophene).[35−37] There is a (010) reflection located at 1.71 Å^{-1}, corresponding to a $\pi-\pi$ stacking distance of ∼3.7 Å, about 0.2 Å shorter than typically observed in P3HT, but similar to other thiophene based polymers such as poly[5,5′-bis(3-dodecyl-2-thienyl)-2,2′-bithiophene] (PQT-12).[38] The intensity distribution of the side chain stacking (h00) peaks suggests a bimodal distribution of crystallite orientations, in this case, two main populations of

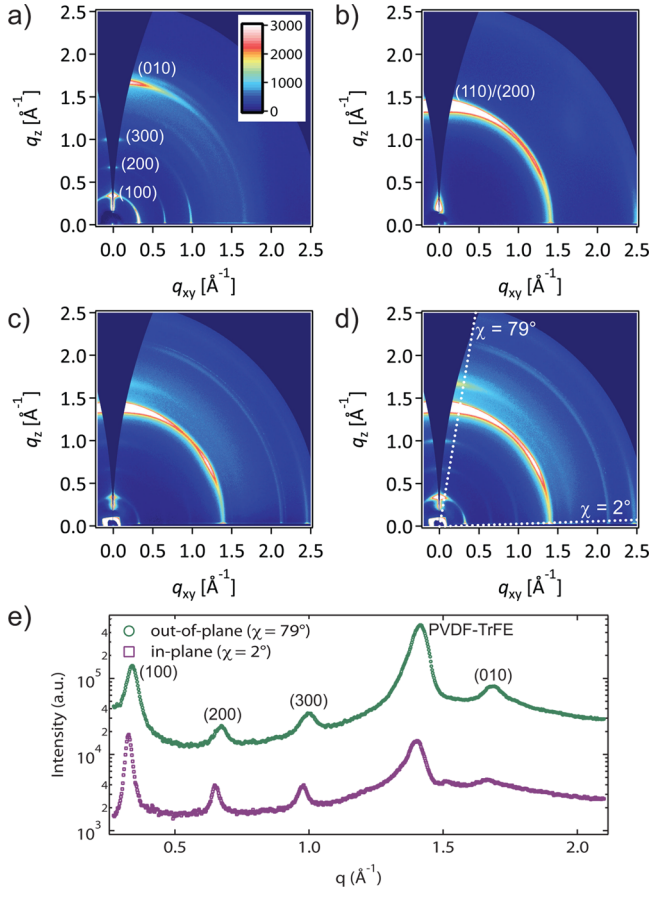

Figure 3. Two-dimensional GIWAXS images of (a) pristine P3EPT, (b) pristine PVDF-TrFE, (c) a 10:90 P3EPT:PVDF-TrFE blend, and (d) a 20:80 P3EPT:PVDF-TrFE blend. The missing wedge along q_z represents the inaccessible region of the Ewald sphere in grazing incidence geometry.[39] Line-cut profiles at specific polar angles (χ) for the 20:80 blend are shown in (e). The profile at χ = 79° represents the scattering in the nearly out-of-plane direction, and the profile at χ = 2° represents scattering in the in-plane direction.

dx.doi.org/10.1021/mz5005647 | ACS Macro Lett. 2014, 3, 1244−1248

crystallites that are either edge-on or face-on. This is seen based on the enhancement of intensity in both the nearly out-of-plane direction (along q_z) and the in-plane direction (along q_{xy}) for all three side chain stacking reflections. The (010) reflection shows the greatest intensity in the nearly out-of-plane direction, suggesting a relatively greater amount of face-on crystallites compared to other orientations. However, it is expected that the crystallite orientations determined from the $\pi-\pi$ stacking reflection should match that of the side chain stacking reflection, that is, the (010) peak should also show a bimodal distribution of orientations. This discrepancy could be a result of imperfect registry, for example, slight changes in tilt angle, among molecules composing edge-on crystallites that disrupt $\pi-\pi$ stacking but do not affect the side chain stacking distance.

In the P3EPT:PVDF-TrFE blend films, scattering features from both components are present and similar to their respective scattering patterns in the single component films. This trend persists for blends of varying P3EPT composition, as shown in both the 2D GIWAXS images (Figure 3c,d) and the line cuts along the nearly out-of-plane and in-plane directions (Figure 3e). The two regions of high intensity in the (h00) peaks of P3EPT that indicate bimodal crystallite distribution are also seen in the blend films, especially at higher P3EPT fraction, for example, a 35:65 P3EPT:PVDF-TrFE blend, as shown in the Supporting Information. This suggests that the two polymers maintain their crystallinity when blended together, and the crystallites in the blend film are composed of either P3EPT or PVDF-TrFE. This is not surprising assuming that the polymers phase separate and form relatively distinct semicrystalline P3EPT and PVDF-TrFE domains, which is needed for functioning resistive switches. However, it is possible that some mixed amorphous regions exist, but this cannot be probed with GIWAXS.

The GIWAXS results show that alteration of polythiophene side chain structure can impact key features of the morphology, such as crystallite orientation and domain size. This opens up new avenues to explore the effect of semiconductor crystallite orientation on the performance of polymer ferroelectric resistive switches, and P3EPT shows promise as a semiconducting polymer where crystallite orientation can be tuned by changing simple processing or deposition methods.

In addition to the smaller phase separation length scales and high crystallinity that can be achieved with P3EPT compared to the less crystalline, regio-irregular polythiophene with hydrocarbon side chains (rir-P3HT), P3EPT can be easily incorporated into all-organic ferroelectric switches, as shown in Figure 4. A memory device must have distinct ON and OFF states, and Figure 4 reveals that P3EPT:PVDF-TrFE results in a much higher current density in the positively poled ON state compared to the negatively poled OFF state. The poling voltage used was ±20 V, corresponding to a field of about 10^8 V/m, similar to previous work.[18] P3EPT:PVDF-TrFE devices also show reasonable ON/OFF ratios (52 for a 10% P3EPT blend measured at 3 V). Successful devices were fabricated out of P3EPT:PVDF-TrFE blends ranging from 10 to 50% P3EPT (Supporting Information). This highlights the potential versatility of blends of P3EPT with PVDF-TrFE and one of the benefits resulting from overall smaller dimensions of phase separation, as previous work using rir-P3HT only reported working devices with up to 10% rir-P3HT.[18] The current density (read at 3 V) of a device initially poled to the ON state then held at 0 V, decreased from about 2 A/m^2 shortly after poling to about 0.1 A/m^2 14 h later, demonstrating reasonable

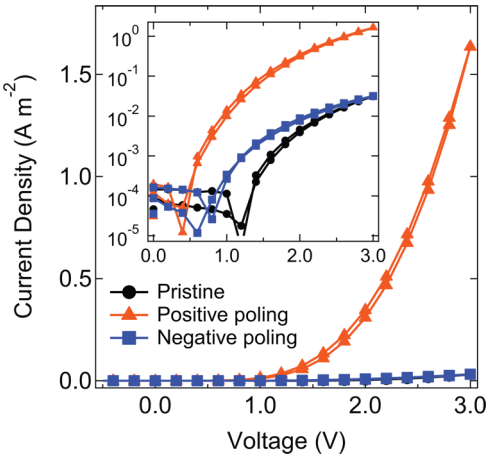

Figure 4. Electrical characteristics of ferroelectric resistive switches fabricated from a 10:90 P3EPT:PVDF-TrFE polymer blend. The device structure used was glass/ITO/P3EPT:PVDF-TrFE(~200 nm)/Ca(10 nm)/Al(90 nm). Devices were poled with a ±20 V pulse. The current−voltage behavior is shown and it is clear that the positively poled ON state has greater current density compared to the negatively poled OFF state. Pristine refers to the device before any poling was applied. A semilog plot is shown in the inset.

retention times for these initial devices (Supporting Information). Future work will determine the best performing electrode layers for this materials system to optimize the switching and retention characteristics.

Our work has shown that side chain modification of a semiconducting polymer can drastically change the phase separation of semiconductor-ferroelectric polymer blends. Specifically, compared to a polythiophene with a hydrocarbon side chain such as P3HT, a polythiophene with a side chain structure containing an ester functional group, P3EPT, results in smaller domain sizes and excellent domain size tunability when blended with the common ferroelectric polymer PVDF-TrFE. This is a significant improvement towards realizing an ideal morphology for all-polymer ferroelectric resistive switches. P3EPT shows signatures of strong crystallinity, and its crystallites adopt a relatively bimodal distribution of edge-on and face-on orientations when spun cast. Furthermore, P3EPT:PVDF-TrFE blends produce working ferroelectric resistive switches over a range of P3EPT weight fractions with good ON/OFF ratios. This material provides a potential model system to understand fundamental effects of semiconductor domain size, crystallinity, and crystallite orientation on electrical properties for organic resistive switches. These studies provide insights into the subtleties of the effects of polymer side chain structure on polymer−polymer interactions, applicable to both the physics of ferroelectric−semiconductor polymer blends, in general, and the improvement of organic memory devices.

■ ASSOCIATED CONTENT

Ⓢ Supporting Information

Experimental details and additional characterization data. This material is available free of charge via the Internet at http://pubs.acs.org.

■ AUTHOR INFORMATION

Corresponding Author

*E-mail: mchabinyc@engineering.ucsb.edu.

Notes

The authors declare no competing financial interest.

■ ACKNOWLEDGMENTS

This work was supported by the Air Force Office of Scientific Research (AFOSR) under the MURI Grant FA9550-12-1-0038. G.M.S. received additional support from the National Science Foundation Graduate Research Fellowship Program (DGE-1144085). The MRL Shared Experimental Facilities are supported by the MRSEC Program of the NSF under Award No. DMR 1121053; a member of the NSF-funded Materials Research Facilities Network (www.mrfn.org). Portions of this research were carried out at the Stanford Synchrotron Radiation Lightsource, a Directorate of SLAC National Accelerator Laboratory and an Office of Science User Facility operated for the U.S. Department of Energy Office of Science by Stanford University.

■ REFERENCES

(1) He, M.; Qiu, F.; Lin, Z. *Energy Environ. Sci.* **2013**, *6*, 1352−1361.
(2) Holliday, S.; Donaghey, J. E.; McCulloch, I. *Chem. Mater.* **2014**, *26*, 647−663.
(3) Arias, A. C.; MacKenzie, J. D.; McCulloch, I.; Rivnay, J.; Salleo, A. *Chem. Rev.* **2010**, *110*, 3−24.
(4) Facchetti, A. *Chem. Mater.* **2011**, *23*, 733−758.
(5) Dou, L.; You, J.; Hong, Z.; Xu, Z.; Li, G.; Street, R. A.; Yang, Y. *Adv. Mater.* **2013**, *25*, 6642−6671.
(6) Asadi, K.; de Bruyn, P.; Blom, P. W. M.; de Leeuw, D. M. *Appl. Phys. Lett.* **2011**, *98*, 183301.
(7) Yuan, Y.; Xiao, Z.; Yang, B.; Huang, J. *J. Mater. Chem. A* **2014**, *2*, 6027−6041.
(8) Yuan, Y.; Reece, T. J.; Sharma, P.; Poddar, S.; Ducharme, S.; Gruverman, A.; Yang, Y.; Huang, J. *Nat. Mater.* **2011**, *10*, 296−302.
(9) Yuan, Y.; Sharma, P.; Xiao, Z.; Poddar, S.; Gruverman, A.; Ducharme, S.; Huang, J. *Energy Environ. Sci.* **2012**, *5*, 8558−8563.
(10) Nalwa, K. S.; Carr, J. A.; Mahadevapuram, R. C.; Kodali, H. K.; Bose, S.; Chen, Y.; Petrich, J. W.; Ganapathysubramanian, B.; Chaudhary, S. *Energy Environ. Sci.* **2012**, *5*, 7042−7049.
(11) Heremans, P.; Gelinck, G. H.; Müller, R.; Baeg, K.-J.; Kim, D.-Y.; Noh, Y.-Y. *Chem. Mater.* **2011**, *23*, 341−358.
(12) Han, S.-T.; Zhou, Y.; Roy, V. A. L. *Adv. Mater.* **2013**, *25*, 5425−5449.
(13) Ling, Q.-D.; Liaw, D.-J.; Zhu, C.; Chan, D. S.-H.; Kang, E.-T.; Neoh, K.-G. *Prog. Polym. Sci.* **2008**, *33*, 917−978.
(14) Naber, R. C. G.; Asadi, K.; Blom, P. W. M.; de Leeuw, D. M.; de Boer, B. *Adv. Mater.* **2010**, *22*, 933−945.
(15) Asadi, K.; Li, M.; Blom, P. W.; Kemerink, M.; de Leeuw, D. M. *Mater. Today* **2011**, *14*, 592−599.
(16) Lovinger, A. J. *Science* **1983**, *220*, 1115−1121.
(17) Baltá Calleja, F.; Arche, A.; Ezquerra, T.; Cruz, C.; Batallán, F.; Frick, B.; Cabarcos, E. In Structure in Polymers with Special Properties. In *Adv. Polym. Sci.*; Zachmann, H.-G., Ed.; Springer: Berlin, Heidelberg, 1993; Vol. *108*; pp 1−48.
(18) Asadi, K.; de Leeuw, D. M.; de Boer, B.; Blom, P. W. M. *Nat. Mater.* **2008**, *7*, 547−550.
(19) Asadi, K.; de Boer, T. G.; Blom, P. W. M.; de Leeuw, D. M. *Adv. Funct. Mater.* **2009**, *19*, 3173−3178.
(20) Kemerink, M.; Asadi, K.; Blom, P. W.; de Leeuw, D. M. *Org. Electron.* **2012**, *13*, 147−152.
(21) Khikhlovskyi, V.; Wang, R.; van Breemen, A. J. J. M.; Gelinck, G. H.; Janssen, R. A. J.; Kemerink, M. *J. Phys. Chem. C* **2014**, *118*, 3305−3312.
(22) Asadi, K.; Wondergem, H. J.; Moghaddam, R. S.; McNeill, C. R.; Stingelin, N.; Noheda, B.; Blom, P. W. M.; de Leeuw, D. M. *Adv. Funct. Mater.* **2011**, *21*, 1887−1894.
(23) Nougaret, L.; Kassa, H. G.; Cai, R.; Patois, T.; Nysten, B.; van Breemen, A. J. J. M.; Gelinck, G. H.; de Leeuw, D. M.; Marrani, A.; Hu, Z.; Jonas, A. M. *ACS Nano* **2014**, *8*, 3498−3505.
(24) Li, M.; Stingelin, N.; Michels, J. J.; Spijkman, M.-J.; Asadi, K.; Beerends, R.; Biscarini, F.; Blom, P. W. M.; de Leeuw, D. M. *Adv. Funct. Mater.* **2012**, *22*, 2750−2757.
(25) Khan, M. A.; Bhansali, U. S.; Almadhoun, M. N.; Odeh, I. N.; Cha, D.; Alshareef, H. N. *Adv. Funct. Mater.* **2013**, *24*, 1372−1381.
(26) Noland, J. S.; Hsu, N. N.-C.; Saxon, R.; Schmitt, J. M. Multicomponent Polymer Systems. *Adv. Chem. Ser.*; American Chemical Society: Washington, DC, 1971; Vol. *99*; Chapter 3, pp 15−28.
(27) Li, M.; Stingelin, N.; Michels, J. J.; Spijkman, M.-J.; Asadi, K.; Feldman, K.; Blom, P. W. M.; de Leeuw, D. M. *Macromolecules* **2012**, *45*, 7477−7485.
(28) Li, M.; Wondergem, H. J.; Spijkman, M.-J.; Asadi, K.; Katsouras, I.; Blom, P. W. M.; de Leeuw, D. M. *Nat. Mater.* **2013**, *12*, 433−438.
(29) Kang, S. J.; Park, Y. J.; Sung, J.; Jo, P. S.; Park, C.; Kim, K. J.; Cho, B. O. *Appl. Phys. Lett.* **2008**, *92*, 012921.
(30) Kang, S. J.; Park, Y. J.; Bae, I.; Kim, K. J.; Kim, H.-C.; Bauer, S.; Thomas, E. L.; Park, C. *Adv. Funct. Mater.* **2009**, *19*, 2812−2818.
(31) Ho, V.; Boudouris, B. W.; Segalman, R. A. *Macromolecules* **2010**, *43*, 7895−7899.
(32) Prosa, T. J.; Winokur, M. J.; McCullough, R. D. *Macromolecules* **1996**, *29*, 3654−3656.
(33) Su, G. M.; Pho, T. V.; Eisenmenger, N. D.; Wang, C.; Wudl, F.; Kramer, E. J.; Chabinyc, M. L. *J. Mater. Chem. A* **2014**, *2*, 1781−1789.
(34) Jung, H. J.; Chang, J.; Park, Y. J.; Kang, S. J.; Lotz, B.; Huh, J.; Park, C. *Macromolecules* **2009**, *42*, 4148−4154.
(35) Causin, V.; Marega, C.; Marigo, A.; Valentini, L.; Kenny, J. M. *Macromolecules* **2005**, *38*, 409−415.
(36) Prosa, T. J.; Winokur, M. J.; Moulton, J.; Smith, P.; Heeger, A. J. *Macromolecules* **1992**, *25*, 4364−4372.
(37) Xiao, X.; Hu, Z.; Wang, Z.; He, T. *J. Phys. Chem. B* **2009**, *113*, 14604−14610.
(38) Jimison, L. H.; Salleo, A.; Chabinyc, M. L.; Bernstein, D. P.; Toney, M. F. *Phys. Rev. B* **2008**, *78*, 125319.
(39) Baker, J. L.; Jimison, L. H.; Mannsfeld, S.; Volkman, S.; Yin, S.; Subramanian, V.; Salleo, A.; Alivisatos, A. P.; Toney, M. F. *Langmuir* **2010**, *26*, 9146−9151.